

**Graded-Bandgap AlGaAs Solar Cells for AlGaAs/Ge Cascade Cells\***

M.L. Timmons, R. Venkatasubramanian, T.S. Colpitts, J.S. Hills and J.A. Hutchby  
*Research Triangle Institute  
 Research Triangle Park, NC*

P.A. Iles and C.L. Chu  
*Applied Solar Energy Corporation  
 City of Industry, CA*

P/N graded-bandgap  $\text{Al}_x\text{Ga}_{(1-x)}\text{As}$  solar cells have been fabricated and show AM0 conversion efficiencies in excess of 15 percent without AR coatings. The emitters of these cells are graded between  $0.08 \leq x \leq 0.20$  during growth of 0.25- to 0.30- $\mu\text{m}$ -thick layers. The keys to achieving this performance have been careful selection of organometallic sources and scrubbing oxygen and water vapor from the  $\text{AsH}_3$  source. Source selection and growth has been optimized using time-resolved photoluminescence. Preliminary radiation-resistance measurements show AlGaAs cells degraded less than GaAs cells at high 1-MeV electron fluences, and AlGaAs cells grown on GaAs and Ge substrates degrade comparably.

**Introduction**

Bandgap grading in the emitters of AlGaAs/GaAs solar cells is an attractive method for improving minority-carrier collection. The bandgap gradient creates an electric field that, according to the modeling of Hutchby and Fudurich [ref. 1], allows 80- and 97-percent reductions in bulk and surface hole recombinations, respectively. Reducing these losses substantially increases the "blue" response of cells. Compositional grading of emitters is also thought to increase radiation resistance, an important factor for cells intended for use in space. Experimentally, though, the predicted benefits of bandgap grading have not been fully realized. For example, Wagner and Shealy reported almost identical performance for graded-bandgap and a heteroface cells with neither outperforming homojunctions [ref. 2]. Reports on the radiation resistance of graded-bandgap AlGaAs cells are very sparse, if they exist at all.

In this paper, we present results for the growth, fabrication, and characterization of graded-emitter AlGaAs cells grown on  $\text{Al}_{0.08}\text{Ga}_{0.92}\text{As}$  base layers. This structure is a candidate component (along with  $\text{Al}_{0.08}\text{Ga}_{0.92}\text{As}$  homojunctions or  $\text{Al}_x\text{Ga}_{(1-x)}\text{As}$ - $\text{Al}_{0.08}\text{Ga}_{0.92}\text{As}$  heteroface cells) of an AlGaAs/Ge cascade cell that offers close current matching between the top and bottom cells under AM0 conditions. Radiation-resistance measurements have been made on nonoptimized AlGaAs graded-bandgap cells, and these data are also included.

\* This work funded by the U.S. Air Force under Contract No. F33615-87-C-2804. Contents of this paper have been cleared for release at this meeting.

## Material Growth and Cell Fabrication

The AlGaAs growth was carried out at atmospheric pressure by organometallic vapor phase epitaxy (OMVPE). Trimethylgallium (TMG), trimethylaluminum (TMA), and arsine ( $\text{AsH}_3$ ) in a 10-percent mixture diluted with  $\text{H}_2$ , were the Ga, Al, and As sources, respectively. Zinc (Zn) from diethylzinc (DEZ) and selenium (Se) from hydrogen selenide ( $\text{H}_2\text{Se}$ ) were the p- and n-type dopants, respectively. During the growths the V/III ratio was kept between 30 and 40, and growth rates of about  $0.1 \mu\text{m}/\text{min}$  were used. When graded layers were required, the  $\text{H}_2$  flows through both the TMG and TMA bubblers were controlled by a computer to keep the growth rates approximately constant, yielding reproducible linear grading.

Material quality is the cornerstone of any good solar cell, and  $\text{Al}_x\text{Ga}_{(1-x)}\text{As}$  is particularly difficult to grow even at compositions as low as  $x=0.10$ . In earlier work, we showed that minority-carrier lifetimes, determined from time-resolved photoluminescence (TPL), can decrease relative to GaAs by factors of 3 and 10 in  $\text{Al}_{0.1}\text{Ga}_{0.9}\text{As}$  and  $\text{Al}_{0.2}\text{Ga}_{0.8}\text{As}$ , respectively, even for moderately high growth temperatures ( $750$  to  $770^\circ\text{C}$ ) [ref. 3]. Therefore, optimizing the AlGaAs growth has been a key factor in achieving good cell results. Optimization has relied upon TPL lifetime measurements, performed under the direction of Dr. R.K. Ahrenkiel of the Solar Energy Research Institute, and cell performance. Using these techniques, we have been able to screen TMA and TMG sources and select ones that yield long minority-carrier lifetimes. The current TMA and TMG sources were provided by American Cyanamid and Eagle-Picher, respectively.

The quality of the  $\text{AsH}_3$  is the second factor that needed scrutiny. During this work, an oxygen and water-vapor scavenger, marketed by Millipore Corp., was evaluated for the  $\text{AsH}_3$ . This unit resulted immediately in significant increases in the PL intensity from  $\text{Al}_{0.08}\text{Ga}_{0.92}\text{As}$  double heterojunctions when the growth temperature was  $780^\circ\text{C}$ . At lower temperatures, the increases are even greater. The minority-carrier lifetimes in  $\text{Al}_{0.08}\text{Ga}_{0.92}\text{As}$  grown with this oxygen and water-vapor scrubber have been as much as 50 percent greater ( $\sim 67$  versus  $\sim 42$  ns) for growth at  $780^\circ\text{C}$  compared to growth without scrubber use.

At the device level, these factors—good quality TMA and TMG sources and  $\text{AsH}_3$  scrubbing—have permitted us to grow  $\text{Al}_{0.08}\text{Ga}_{0.92}\text{As}$  homojunction cells recently at  $725^\circ\text{C}$  that perform almost as well as those grown previously at  $780^\circ\text{C}$ . This will be discussed in more detail below.

All the cells fabricated during this program have used standard processing. A typical device structure is shown in Figure 1. Hall measurements and C-V analyses, using individually grown layers on semi-insulating GaAs substrates, have yielded the following data:

1. the base carrier concentrations are about  $3 \times 10^{17} \text{ cm}^{-3}$ ,
2. the emitter carrier concentrations are  $1\text{-}3 \times 10^{18} \text{ cm}^{-3}$ , and
3. carrier concentrations in the GaAs caps are about  $8\text{-}10 \times 10^{18} \text{ cm}^{-3}$ .

Carrier concentrations in  $\text{Al}_{0.88}\text{Ga}_{0.12}\text{As}$  window layers are low ( $\sim 10^{17} \text{ cm}^{-3}$ ) when grown at  $780^\circ\text{C}$  with Zn doping, but by lowering growth temperatures for the windows to  $700^\circ\text{C}$ , values above  $10^{18} \text{ cm}^{-3}$  have been achieved. Reducing the growth temperature for the window and cap layers improved cell fill factors.

The interface recombination velocity  $S$  between the  $\text{Al}_{0.88}\text{Ga}_{0.12}\text{As}$  window layer and the AlGaAs emitter is high. Using TPL to examine  $\text{Al}_{0.88}\text{Ga}_{0.12}\text{As}/\text{Al}_{0.08}\text{Ga}_{0.92}\text{As}$ , we have estimated values for  $S$  as large as  $3 \times 10^4 \text{ cm/s}$  in spite of high growth temperatures ( $\sim 780^\circ\text{C}$ ) [ref. 4]. Values of  $S$  of this magnitude have recently been reported by Ahrenkiel et al. for AlGaAs/GaAs interfaces grown at  $700^\circ\text{C}$  [ref. 5]. Our data indicate higher  $S$  values for AlGaAs/AlGaAs interfaces that may require additional passivation. This will be addressed in future work.

## Cell Characterization

The graded emitter has been characterized and optimized in grown structures based on cell performance. At the beginning of the program, the intent was to compositionally grade the  $\text{Al}_x\text{Ga}_{(1-x)}\text{As}$  in the emitter from  $x=0.08$  to  $x=0.30$  while growing a  $0.5\text{-}\mu\text{m}$ -thick layer. Emitters with values of  $x$  greater than  $x \simeq 0.3$  have also been examined. The spectral responses from several cells are shown in Figure 2. The compositions at the end of the emitter grading are  $x=0.3$ ,  $0.45$ , and  $0.6$  for these cells, and emitter thicknesses are about  $0.35 \mu\text{m}$ , except for one (Sample No. 447) that has a  $0.5\text{-}\mu\text{m}$ -thick layer. The short-wavelength response decreases as the Al concentration increases even for the thin,  $0.35\text{-}\mu\text{m}$  emitters. This shows that the reduction in minority-carrier lifetime that accompanies the increasing Al content outweighs the field-induced advantages that come from grading, and many carriers generated in the surface region are not being collected. Even with limiting the endpoint of the graded composition to  $\text{Al}_{0.3}\text{Ga}_{0.7}\text{As}$ , graded-emitter cells show only marginal improvement relative to homojunction  $\text{Al}_{0.08}\text{Ga}_{0.92}\text{As}$  cells with comparable emitter thicknesses. This is illustrated in Figure 3 where the dark and illuminated I-V characteristics of a homojunction cell and a cell graded to  $x=0.3$  are displayed. The graded-cell efficiency (11.9 percent) was the best during the early phase of program but has only a 1-percent efficiency advantage over a shallow homojunction that is typical of the homojunction cells (best homojunction cell grown during this period has a 13.6-percent conversion efficiency with no AR coating).

Since the homojunctions continued to outperform the graded-emitter junctions with  $x=0.3$  at the end of the grading, reduced minority-carrier lifetimes, coupled

with possible large interface recombination velocities, appeared to negate the advantages that were hoped for the graded emitters. Grading an  $\text{Al}_x\text{Ga}_{(1-x)}\text{As}$  layer from  $0.08 \leq x \leq 0.3$  over  $0.5 \mu\text{m}$  produces an electric field of about  $5300 \text{ V/cm}$ , and a layer graded from  $0.08 \leq x \leq 0.18$  over  $0.30 \mu\text{m}$  contains a field of about  $4700 \text{ V/cm}$ . This latter layer, though, will have a minority-carrier lifetime that is between 3 and 10 times longer than in the former while sacrificing only about 25 percent of the desired field. Therefore, the emitter-grading limits and thicknesses were reduced to  $0.08 \leq x \leq 0.18$  and  $0.25$  to  $0.3 \mu\text{m}$ , respectively. These values have become the guidelines for current cell growth.

As the quality of the AlGaAs has improved, cell efficiencies have also increased. The scrubbing described above for the  $\text{AsH}_3$  resulted in step-like increases in cell efficiencies. The I-V characteristic of one of the first graded-bandgap cells (Sample No. 492) grown using the scrubber-and the reduced grading composition-is shown in Figure 4; this cell has a power conversion efficiency of 15.3 percent without an AR coating. The  $\text{Al}_x\text{Ga}_{(1-x)}\text{As}$  emitter composition varied from  $0.08 \leq x \leq 0.18$  over  $0.25 \mu\text{m}$  of emitter material. In Figure 5, the spectral response of Sample No. 492 is compared to a cell (Sample No. 482) with a  $\text{Al}_{0.08}\text{Ga}_{0.92}\text{As}$  homojunction ( $0.2\text{-}\mu\text{m}$ -thick emitter) that was grown without use of the  $\text{AsH}_3$  scrubber, and a cell (Sample No. 494) graded from  $0.08 \leq x \leq 0.18$  during growth of a  $0.6\text{-}\mu\text{m}$ -thick emitter. The short-wavelength response of Sample No. 492 is significantly improved compared to either of the other two samples. The response difference between 492 and 494 is somewhat surprising and shows that many of the carriers generated at the surface in sample 494 are still not being collected. With a good AR coating, cell 492 projects a efficiency between 18.5 and 19.5 percent, which is very close to our maximum modeled value for this composition .

Graded-bandgap cells have also been compared to two kinds of heteroface cells. Sample No. 563, whose I-V characteristic is shown in Figure 6, contains a  $0.4\text{-}\mu\text{m}$ -thick,  $\text{Al}_{0.18}\text{Ga}_{0.82}\text{As}$  emitter. For this sample  $V_{oc}$  equals  $1.081 \text{ V}$ ,  $J_{sc}$  equals  $28.03 \text{ mA/cm}^2$  (active-area), and the fill factor is 0.82 yielding an active-area efficiency of 17.9% (cell has a single-layer  $\text{Si}_3\text{N}_4$  AR coating). Comparison has also been made with a cell (Sample No. 564) containing an emitter consisting of three different  $\text{Al}_x\text{Ga}_{(1-x)}\text{As}$  layers,  $0.10 \mu\text{m}$  of  $\text{Al}_{0.08}\text{Ga}_{0.92}\text{As}$ ,  $0.10 \mu\text{m}$  of  $\text{Al}_{0.13}\text{Ga}_{0.87}\text{As}$ , and  $0.1 \mu\text{m}$  of  $\text{Al}_{0.18}\text{Ga}_{0.82}\text{As}$ . The I-V characteristic for this cell is also shown in Figure 6, and  $J_{sc}$ ,  $V_{oc}$ , and fill factor are  $24.2 \text{ mA/cm}^2$ ,  $1.056 \text{ V}$ , and 0.78, respectively, for an active-area efficiency of 14.7% (no AR coating). The efficiency of this cell projects to about 18.5 percent with a coating and, based on the results of our study of AlGaAs/AlGaAs interfaces [ref. 4], may be benefiting from a reduction in S.

The cells described above were grown at  $780$  to  $800^\circ\text{C}$ . One of the most encouraging recent developments is the growth of AlGaAs cells at  $725^\circ\text{C}$ . The I-V characteristic of two of these cells (Sample Nos. 566 and 567) are shown in Figure 7 and are comparable to cells grown at  $780^\circ\text{C}$ ; sample 566 is an  $\text{Al}_{0.08}\text{Ga}_{0.92}\text{As}$  homojunction, and

sample 567 contains a graded emitter ( $0.08 \leq x \leq 0.18$ ). Both emitters are about  $0.25 \mu\text{m}$  thick, and cell performances of the two devices are almost identical— $J_{\text{sc}} \simeq 26 \text{ mA/cm}^2$ ,  $V_{\text{oc}} \simeq 1.02 \text{ V}$  and fill factor  $\simeq 0.78$ —with active-area efficiencies of about 15.2 percent (no AR coating). The spectral responses from the two cells are also very comparable to each other and to cells grown at higher temperatures.

Considering all of the cell data, it appears that, as long as the AlGaAs quality is very high and limited to  $x \leq 0.2$  and that the emitter is thin ( $\sim 0.3$ ), the details of emitter growth are not as critical as we originally suspected. The similar performances of the different structures described above support this conclusion. Therefore, it will likely be other factors, radiation resistance, for example, that will determine the optimum top-cell structure in the AlGaAs/Ge cascade cell.

### Radiation Resistance

AlGaAs cells with different types of emitters were exposed to 1-MeV electrons at fluences of  $5 \times 10^{14}$ ,  $1 \times 10^{15}$ , and  $5 \times 10^{15} \text{ cm}^{-2}$  to begin determining the radiation-resistance properties of the cells. Cells with the following six types of emitters have been irradiated at the JPL facility:

1. homojunction  $\text{Al}_{0.08}\text{Ga}_{0.92}\text{As}$  cells with  $\sim 0.5\text{-}\mu\text{m}$ -thick emitters,
2. cells with  $0.5\text{-}\mu\text{m}$ -thick emitters graded from  $0.08 \leq x \leq 0.30$  (emitters have a  $0.1\text{-}\mu\text{m}$  thick  $\text{Al}_{0.08}\text{Ga}_{0.92}\text{As}$  spacer before the grading was initiated),
3. heteroface cells with  $\text{Al}_{0.08}\text{Ga}_{0.92}\text{As}$  bases and  $\text{Al}_{0.3}\text{Ga}_{0.7}\text{As}$  emitters ( $0.5 \mu\text{m}$  thick),
4. cells with thick  $\text{Al}_{0.08}\text{Ga}_{0.92}\text{As}$  emitters ( $3\text{-}4 \mu\text{m}$ ),
5. GaAs cells, and
6.  $\text{Al}_{0.08}\text{Ga}_{0.92}\text{As}$  homojunction cells grown on Ge substrates.

Beginning efficiencies for the cells of the first group ( $\text{Al}_{0.08}\text{Ga}_{0.92}\text{As}$  homojunctions) ranged from 14 to 16 percent, the graded-emitter-cell efficiencies of the second group ranged from about 7 to 10 percent, GaAs efficiencies (group 5) were about 17 to 18 percent, and the AlGaAs-on-Ge-cell efficiencies (group 6) were about 14 percent. The remaining two types had lower efficiencies of about 3 and 7 percent for the thick-emitter and heteroface cells, groups 4 and 3, respectively.

In Table 1, data for the fraction of  $V_{\text{oc}}$ ,  $I_{\text{sc}}$  ( $2 \text{ cm} \times 2 \text{ cm}$  cells), and the  $V_{\text{oc}}\text{-}I_{\text{sc}}$  product remaining after exposure of the six cell types to the three fluence levels are presented. Disregarding the data for the thick-emitter cells, which are especially sensitive to diffusion-length reductions, the fraction of the  $V_{\text{oc}}\text{-}I_{\text{sc}}$  product remaining for the lower two fluences,  $5 \times 10^{14}$  and  $1 \times 10^{15} \text{ cm}^{-2}$ , are about the same for the AlGaAs

and GaAs cells, but at the  $5 \times 10^{15} \text{cm}^{-2}$  level, the AlGaAs cells show less degradation than the GaAs. The efficiency of the GaAs cells, however, was initially higher, and it is commonly accepted that lower efficiency cells usually show lower damage. Therefore, the differences may not be as significant as the data would suggest. Also encouraging is the performance of the AlGaAs-on-Ge cells; these devices are no worse than AlGaAs-on-GaAs junctions regarding performance degradation. Finally, at the highest fluence, the data suggest that the graded-emitter structure, although not optimized, outperforms homojunction cells, but initial efficiency differences keep this observation from being more definitive at the present time.

In Table 2, quantum efficiencies (QE) at two wavelengths, 0.5 and 0.8  $\mu\text{m}$ , are presented before and after irradiation at the three fluences. Remaining QE fractions are also indicated. Considering the  $5 \times 10^{15} \text{cm}^{-2}$  fluence and disregarding the data for thick-emitter cells (group 4), the long-wavelength QE degradation, as expected, is greater than the shortwavelength degradation. The AlGaAs-on-Ge cells perform comparably to AlGaAs-on-GaAs cells (groups 1 and 6) at the short wavelength and is slightly better at 0.8  $\mu\text{m}$ , and both have higher QEs than the GaAs cell. The graded-emitter cells (and the heteroface cell) show less short-wavelength degradation and more long-wavelength degradation than either the AlGaAs or GaAs homojunctions.

These data, although not considered definitive, clearly suggest that grading may enhance the radiation resistance of the emitters. These experiments will be repeated using optimum graded-emitter cells that have higher initial efficiencies and will be coupled with deep-level-transient-spectroscopy measurements and TPL determinations of minority-carrier lifetimes.

## Conclusions

In this paper, we have described the growth and characterization of high-quality AlGaAs solar cells that are intended for use as the top cell in the AlGaAs/Ge monolithic cascade cell. Several different emitter structures – homojunction, graded, and heteroface – have been grown. Performances of the best of these cells are approaching practical theoretical limits. Improved material quality is thought to be the key to increased efficiencies. Material growth has been optimized with TPL measurements of minority-carrier lifetime. Graded-bandgap cells ( $0.08 \leq x \leq 0.20$ ) using 0.25- to 0.3- $\mu\text{m}$ -thick emitters have yielded power conversion efficiencies greater than 15 percent without AR coatings.

Preliminary radiation-resistance measurement with 1-MeV electron fluences as great as  $5 \times 10^{15} \text{cm}^{-2}$  have shown AlGaAs cells on GaAs and Ge substrates may degrade less than GaAs cells, and graded emitters (or heteroface cells) may be advantageous for preserving short-wavelength QE response, which is, in fact, a demonstration of one major program goals.

## References

- [ 1. ] J. A. Hutchby and R. L. Fudurich, J. Appl. Phys. **47**, 3140 (1976).
- [ 2. ] D. K. Wagner and J. R. Shealy, Appl. Phys. Lett. **45**, 162, (1984).
- [ 3. ] M. L. Timmons, J. A. Hutchby, R. K. Ahrenkiel and D. J. Dunlavy, *Proceedings of the 15th International Symposium on GaAs and Related Compounds*, 289, Inst. Phys. Conf. Ser. No. 96, Inst. Phys., Bristol (1989).
- [ 4. ] M. L. Timmons, T. S. Colpitts, R. Venkatasubramanian, B. M. Keyes, D. J. Dunlavy, and R. K. Ahrenkiel, "Measurement of AlGaAs/AlGaAs Interface Recombination Velocities", (submitted for publication).
- [ 5. ] R. K. Ahrenkiel, D. J. Dunlavy, B. M. Keyes, S. M. Vernon, T. M. Dixon, S. P. Tobin, K. L. Miller and R. E. Hayes, Appl. Phys. Lett. **55** 1088 (1989).

**Table 1.** Fraction Of Initial  $V_{oc}$ ,  $I_{sc}$ , And  $V_{oc}-I_{sc}$  Product Remaining After Irradiation By 1-MeV Electrons.

Cell Group	$5 \times 10^{14} \text{ cm}^{-2}$			$1 \times 10^{15} \text{ cm}^{-2}$			$5 \times 10^{15} \text{ cm}^{-2}$		
	F ( $V_{oc}$ )	F ( $I_{sc}$ )	F ( $V_{oc} \times I_{sc}$ )	F ( $V_{oc}$ )	F ( $I_{sc}$ )	F ( $V_{oc} \times I_{sc}$ )	F ( $V_{oc}$ )	F ( $I_{sc}$ )	F ( $V_{oc} \times I_{sc}$ )
1. Homojunction (8% E,B on GaAs)	0.93- 0.96	0.91- 0.92	0.85- 0.89	0.92- 0.95	0.88- 0.89	0.81- 0.84	0.87- 0.88	0.63- 0.69	0.57- 0.61
2. Graded Emitter (8-30% E, 8% B)	0.95- 0.97	0.88- 0.91	0.85- 0.88	0.91- 0.95	0.85- 0.88	0.80- 0.82	0.87- 0.94	0.68- 0.76	0.64- 0.70
3. Heteroface (30% E, 8% B)	0.94- 0.97	0.90- 0.91	0.86- 0.88	0.88, 0.93	0.85- 0.87	0.77- 0.79	0.85- 0.87	0.74- 0.75	0.65- 0.66
4. Homojunction (8% Thick-E,B)	0.94- 0.95	0.62- 0.65	0.59- 0.61	0.91- 0.93	0.42- 0.44	0.39- 0.40	0.63	0.09	0.06
5. GaAs	---	---	---	0.91	0.85	0.77	0.83	0.54	0.44
6. Homojunction (8% E,B on Ge)	0.95	0.92	0.88	0.94	0.90	0.84	0.89	0.69	0.61

**Table 2.** Quantum Efficiencies Of AlGaAs Solar Cells At Wavelengths Of 0.5 And 0.8  $\mu\text{m}$  After Irradiation.

Cell Group	Before Irradiation		1-MeV Electron Fluence					
	QE0.5	QE0.8	$5 \times 10^{14} \text{ cm}^{-2}$		$10^{15} \text{ cm}^{-2}$		$5 \times 10^{15} \text{ cm}^{-2}$	
			QE0.5	QE0.8	QE0.5	QE0.8	QE0.5	QE0.8
1. Homojunction (8% E,B on GaAs)	0.88	0.61	0.81 (0.92)	0.47 (0.77)	0.835 (0.95)	0.445 (0.73)	0.635 (0.72)	0.32 (0.52)
2. Graded Emitter (8-30% E, 8% B)	0.80	0.70	0.745 (0.93)	0.355 (0.51)	0.76 (0.95)	0.32 (0.46)	0.73 (0.91)	0.19 (0.27)
3. Heteroface (30% E, 8% B)	0.70	0.445	0.69 (0.98)	0.30 (0.62)	0.68 (0.97)	0.21 (0.44)	0.62 (0.88)	0.15 (0.31)
4. Homojunction (8% thick-E,B)	0.165	0.30	0.09 (0.54)	0.19 (0.64)	0.75 (0.46)	0.185 (0.62)	0.01 (0.06)	0.055 (0.18)
5. GaAs	0.77	0.895	--	--	0.63 (0.82)	0.66 (0.74)	0.43 (0.56)	0.445 (0.50)
6. Homojunction (8% E,B on Ge)	0.895	0.625	--	--	--	--	0.65 (0.72)	0.375 (0.60)

Note: Values in parentheses are fractions of QE remaining after irradiation.



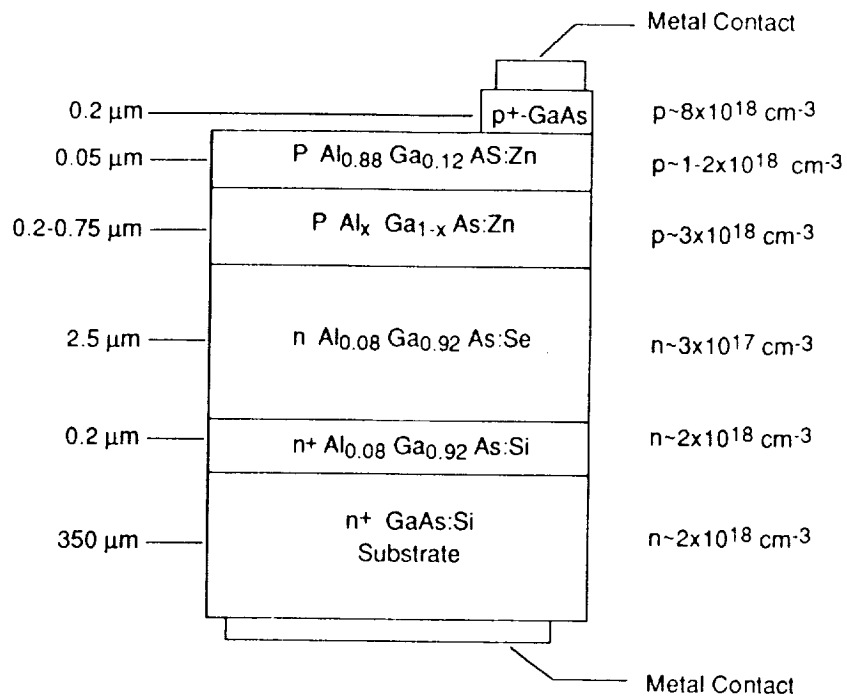


**Figure 1. Schematic diagram of AlGaAs cells being developed for this program. Emitter compositions and thicknesses vary to optimize the structure.**

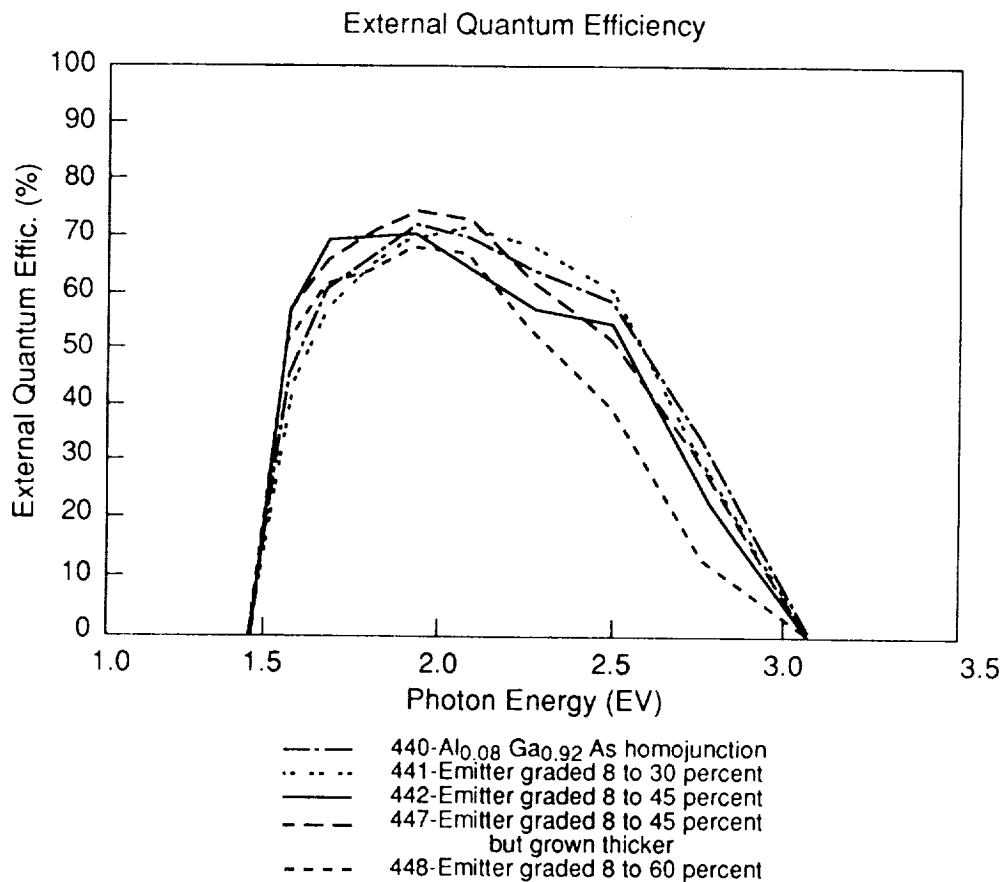
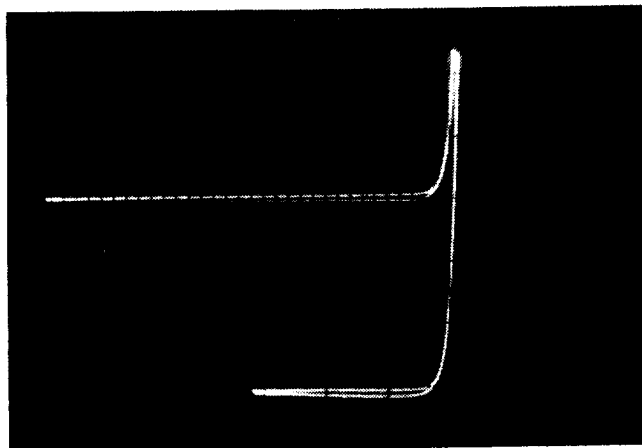
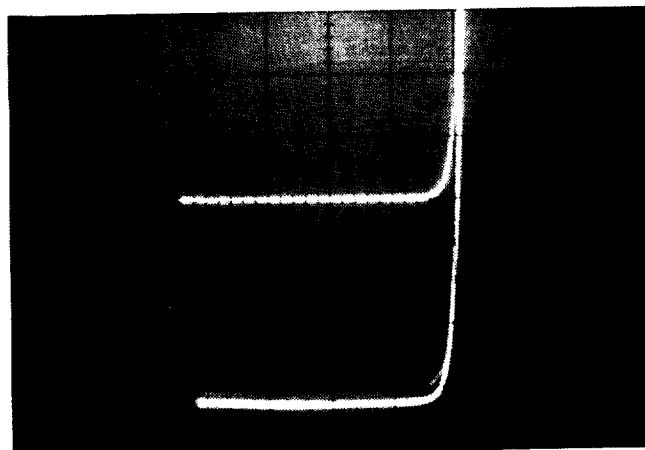


**Figure 2. Spectral responses of five AlGaAs solar cells.**



a) Sample 440 —  $\text{Al}_{0.08}\text{Ga}_{0.92}\text{As}$   
 emitter:  $V_{oc} \sim 1.030 \text{ V}$   
 $J_{sc} \sim 17.0 \text{ mA/cm}^2$   
 $FF \sim 0.83$   
 $\eta \sim 10.7\%$



b) Sample 441 — Graded Bandgap  
 emitter:  $V_{oc} \sim 1.055 \text{ V}$   
 $J_{sc} \sim 18.6 \text{ mA/cm}^2$   
 $FF \sim 0.82$   
 $\eta \sim 11.9\%$

Figure 3. Dark and illuminated I-V characteristics of good  $\text{Al}_{0.08}\text{Ga}_{0.92}\text{As}$ -homojunction and best graded-bandgap cell fabricated during early part of program. Horizontal and vertical scales are 0.5 V and 1 mA, respectively. Efficiencies calculated from active areas of devices (no AR coatings).

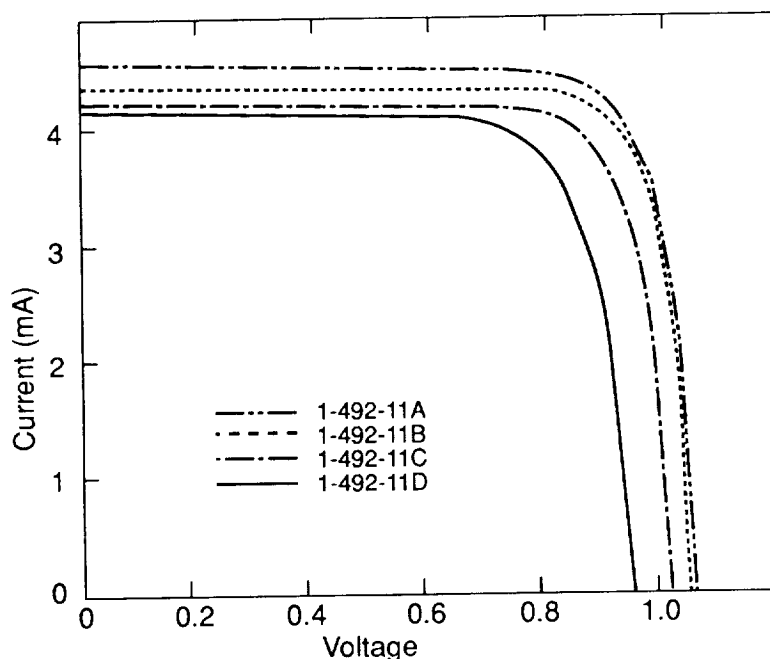
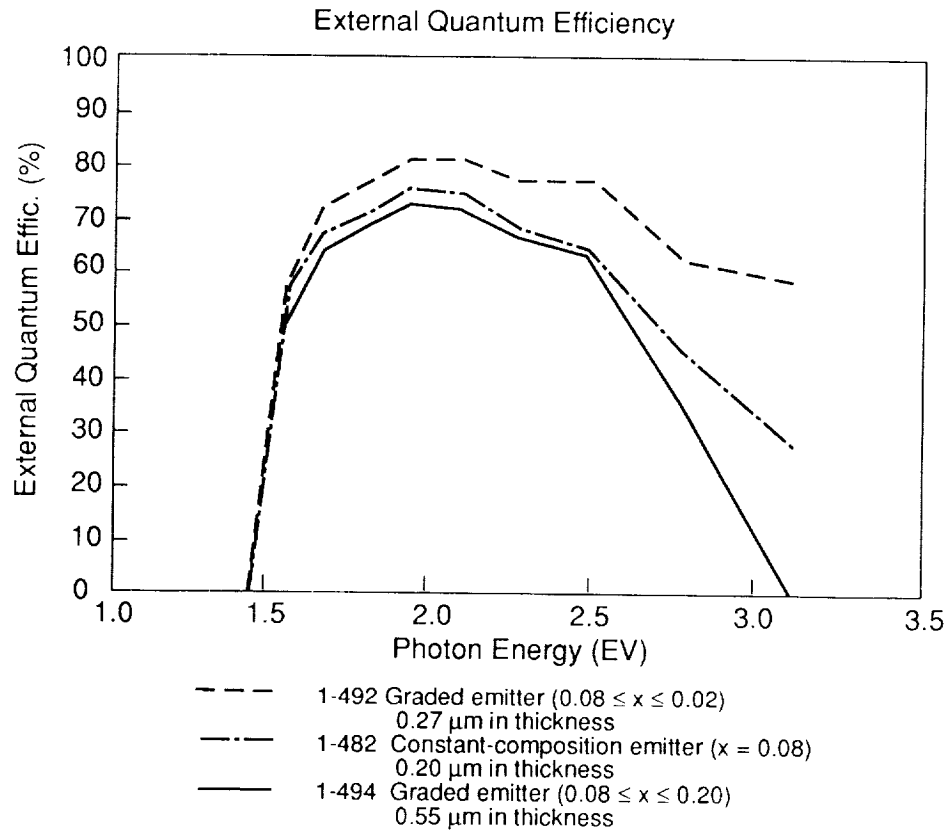
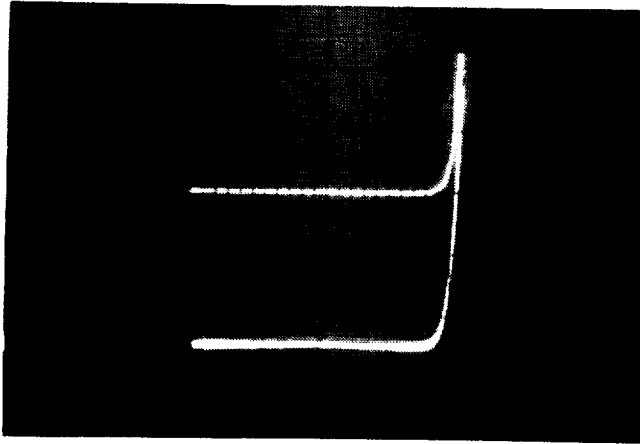


Figure 4. Illuminated I-V characteristics of graded-bandgap AlGaAs solar cells (4 cells fabricated on wafer 1-492). Emitter graded from  $\text{Al}_{0.08}\text{Ga}_{0.92}\text{As}$  to  $\text{Al}_{0.2}\text{Ga}_{0.8}\text{As}$  over  $0.27 \mu\text{m}$ . Best cell:  $V_{oc} = 1.061 \text{ V}$ ,  $J_{sc} = 24.4 \text{ mA/cm}^2$ ,  $FF = 0.81$ ,  $\eta = 15.3\%$  (no AR coating).

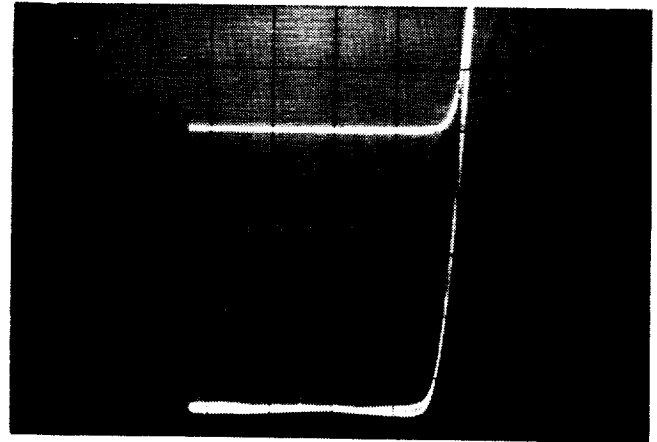


**Figure 5. Spectral responses from several  $\text{Al}_x\text{-Ga}_{(1-x)}\text{As}$  solar cells (no AR coatings).**



a) Sample 563 — Heteroface cell with 0.4- $\mu\text{m}$  thick  $\text{Al}_{0.18}\text{Ga}_{0.82}\text{As}$  emitter:

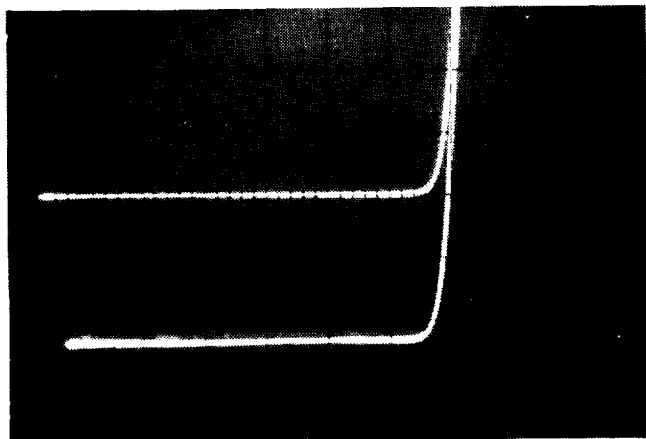
$V_{oc} \sim 1.081 \text{ V}$  (0.5 V/div)  
 $J_{sc} \sim 28.03 \text{ mA/cm}^2$  (2 mA/div)  
 $FF \sim 0.80$   
 $\eta \sim 17.92\%$



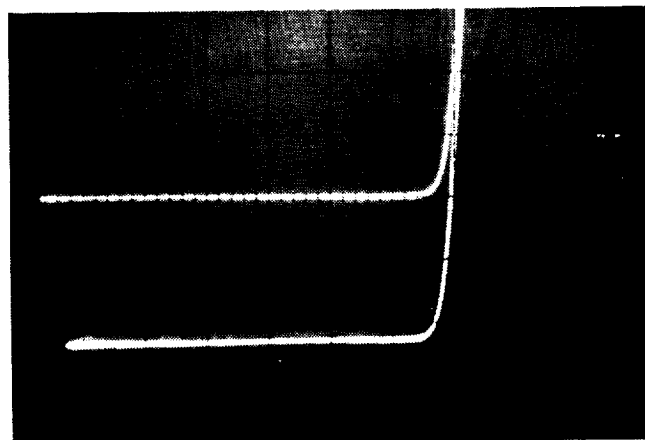
b) Sample 564 — AlGaAs cell with emitter containing 3 Al-concentration step changes:

$V_{oc} \sim 1.056 \text{ V}$  (0.5 V/div)  
 $J_{sc} \sim 24.2 \text{ mA/cm}^2$  (1 mA/div)  
 $FF \sim 0.78$   
 $\eta \sim 14.73\%$

**Figure 6. Dark and illuminated characteristics of AlGaAs cells with step changes in emitter Al concentration: a) single step to  $\text{Al}_{0.18}\text{Ga}_{0.82}\text{As}$ ; b) Al concentration changes from  $\text{Al}_{0.08}\text{Ga}_{0.92}\text{As}$  to  $\text{Al}_{0.13}\text{Ga}_{0.87}\text{As}$  to  $\text{Al}_{0.18}\text{Ga}_{0.82}\text{As}$ . Sample 563 has a single layer of  $\text{Si}_3\text{N}_4$  for an AR coating; sample 564 is uncoated.**



- a) Sample 566 —  $\text{Al}_{0.08}\text{Ga}_{0.92}\text{As}$   
 emitter:  $V_{oc} \sim 1.02 \text{ V}$  (0.5 V/div)  
 $J_{sc} \sim 25.8 \text{ mA/cm}^2$  (2 mA/div)  
 FF  $\sim 0.78$   
 $\eta \sim 15.2 \%$



- b) Sample 567 — Graded Bandgap AlGaAs  
 emitter:  $V_{oc} \sim 1.018 \text{ V}$   
 (0.5 V/div)  
 $J_{sc} \sim 25.7 \text{ mA/cm}^2$  (2 mA/div)  
 FF  $\sim 0.78$   
 $\eta \sim 15.1\%$

**Figure 7. Dark and illuminated I-V characteristic of graded-bandgap and  $\text{Al}_{0.08}\text{Ga}_{0.92}\text{As}$ -homojunction solar cells grown at 725 °C.**